AD NUMBER	
AD360458	
CLASSIFICATION CHANGES	
TO:	unclassified
FROM:	confidential
LIMITATION CHANGES	
TO:	Approved for public release, distribution unlimited
FROM:	Controlling DoD Organization: Defense Nuclear Agency, Washington, DC 20305.
AUTHORITY	
DNA ltr dtd 9 Jun 1982; DNA ltr dtd 9 Jun 1982	

DISCLAIMER NOTICE

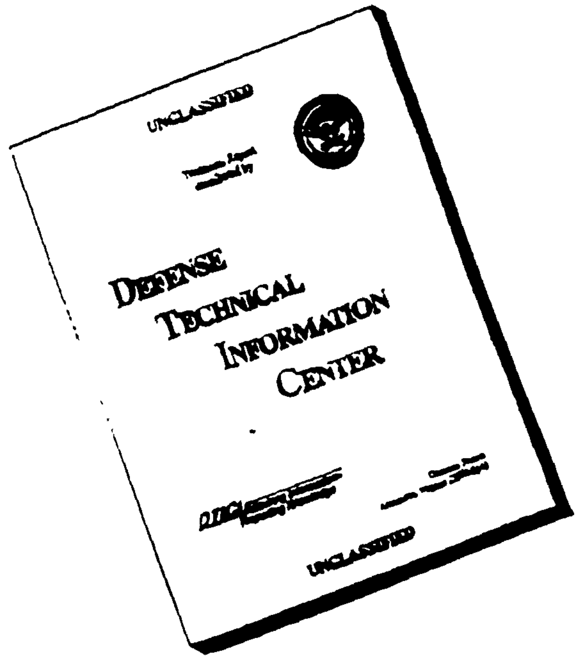

THIS DOCUMENT IS BEST QUALITY AVAILABLE. THE COPY FURNISHED TO DTIC CONTAINED A SIGNIFICANT NUMBER OF PAGES WHICH DO NOT REPRODUCE LEGIBLY.

AD 360458L

DEFENSE DOCUMENTATION CENTER

FOR

SCIENTIFIC AND TECHNICAL INFORMATION

CAMERON STATION ALEXANDRIA. VIRGINIA

[redacted]

WT-1667

This document consists of 42 pages.

No. of 170 copies, Series A

OPERATION

A

360458L

SATELLITE LAUNCHING from AIRCRAFT (U)

Issuance Date: May 2[illegible], 1960

DEFENSE ATOMIC SUPPORT AGENCY
WASHINGTON, D.C.

[redacted]

[redacted]

WT-1667

OPERATION ARGUS

SATELLITE LAUNCHING from AIRCRAFT (U)

Weapons Development Department
U.S. Naval Ordnance Test Station
China Lake, California

[redacted]

ABSTRACT

In the fall of 1957 the Naval Ordnance Test Station (NOTS) was studying the feasibility of launching an observation television satellite from an aircraft. In the spring of 1958, when plans for the Argus experiments were being developed, it was proposed and accepted that the air-launched vehicle under development at NOTS be utilized to place a scintillation counter in polar orbit. This payload was to be used to detect and measure trapped electrons from the nuclear detonations that were to be employed to test the Christofilos theory. The primary instrumentation for the experiments was carried in Explorer IV, and the NOTS satellite payload was to be used as additional, back-up instrumentation.

The vehicle was to be launched at high altitude in a loft maneuver from an interceptor aircraft. The vehicle consisted of a five-stage, unguided, solid-fueled ballistic rocket weighing approximately 2,150 pounds. Ignition of the rocket motors was staged by electronic timers, except for the third stage, which was to be fired at a given angle to the horizon as measured by an infrared telescope. The first two stages of the vehicle were fin-stabilized, and the last three were spin-stabilized. The fifth-stage motor was retro-mounted. The spinning fifth stage, which was to carry the payload, would have acted as a gyroscope and thus maintained orientation in inertial space while coasting around to approximately the antipodal point; at this point the fifth-stage motor, oriented properly with the velocity vector, would have been fired, placing the payload into the desired orbit.

Within the span of 6 months the satellite vehicle and payload were designed, developed, and tested, and six complete systems were manufactured and launched from an F4D-1 aircraft over the Pacific Missile Range. Three orbital attempts employing diagnostic payloads were made in late July and early August 1958, and three final attempts to place the payload in orbit were made on 25, 26, and 28 August 1958.

All firings, except the one on 22 August, malfunctioned during first-stage propulsion. Crystal control of the diagnostic payload transmitter frequency was lost just prior to launch on the 22 August firing. Three possible passes were recorded, but a complete review of the data could not justify an orbital claim.

A world-wide network of microlock stations was built for instrumentation. These stations were located in New Zealand, the Azores, Alaska, Greenland, and China Lake, California. These stations were used to gather International Geophysical Year (IGY) data and to monitor the Explorer IV instrumentation, and were ready to receive if the pilot satellite had been successful.

Although NOTS's efforts on this project were not completely successful, much valuable information was obtained that should be applicable to related projects of the future. In addition to those accomplishments already mentioned, the following are particularly significant:

1. The fly-up aircraft satellite-launch technique was successfully demonstrated. This included outfitting and calibrating two F4D-1 aircraft for launching vehicles and training four pilots in launching techniques. The launching conditions for all full-scale firings were within tolerances, thus the aircraft maneuver reliability and reproducibility were successfully demonstrated.

2. The total structure weight of the vehicle was limited to 5 percent of the overall vehicle weight. This required the development of three new rocket motors with high performance index.

3. An igniter was developed and tested under simulated 180,000-foot altitude.

4. An IBM program for computing vehicle performance, missile tolerances, and ephemerides for satellites from doppler data has been developed. This method of computing ephemerides has been applied to doppler data received from Explorer IV. A six-degrees-of-freedom program study has also been completed for determination of orbital trajectories concurrently with stability studies.

[redacted]

5. In the development, manufacture, and operation of the microlock ground receiver stations an improved capability for rapid frequency scan has been obtained, and these portable stations can now be shipped anywhere in the world and be set into operation within 3 to 4 hours after arrival at the chosen location. The data obtained by the NOTS stations are reported to be among the most useful data that were obtained for IGY and Operation Argus.

6. A 2.3-pound radiation counter and a diagnostic payload of the same weight have been designed, developed, and manufactured. The radiation-counter payloads were used in the last three orbital attempts.

The report documents the development and testing of the aircraft-launched satellite-vehicle system and discusses major component developments and tests.

It is believed that in addition to the contribution made to Operation Argus, the experience gained in this program greatly enhanced the Nation's capabilities in space research and development, and that many of the components developed will find a recurring application in this country's space program.

CONTENTS

[redacted]

SATELLITE LAUNCHING from AIRCRAFT

VEHICLE AND ORBITAL CONCEPT

For certain applications and for launching a relatively small payload, a satellite vehicle launched from an aircraft has many advantages because of its size, relatively low cost, versatility, and general utility. Studies undertaken prior to Operation Argus indicated that a vehicle could be designed which would be inherently simple to manufacture, transport, assemble, check out, and launch. The estimated cost was low, and reliability was believed to be high, since the vehicle would use simple controls and reliable solid-propellant boosters and could be provided with redundant firing circuits.

Figure 1 illustrates the aircraft-launched vehicle as originally conceived and the Argus project team during the early stages of the program.

Table 1 shows the physical characteristics of Stages 1 through 5 of the vehicle.

Figure 2 illustrates the launching concept and the sequence of various stages from aircraft launch to orbit.

The satellite vehicle was to be launched at high altitude in a loft maneuver by an F4D-1 interceptor aircraft. The vehicle was designed to place a 2.3-pound payload in a 1,000-mile orbit. It was a five-stage, unguided, solid-fuel, ballistic rocket which weighed approximately 2,150 pounds. Ignition of the rocket motors was to be staged by metering time with electronic devices except for the third stage, which was fired on an angle to the horizon as measured by an infrared scanner. All stages were to be separated from the previous expended stage by thrust forces at ignition, except for the fifth stage (which was to be disconnected by a small separation charge). The first two propulsion stages were fin-stabilized and the last three were spin-stabilized. The fifth-stage motor was retro-mounted, i.e., its nozzle pointed opposite to the other nozzles. The first four stages of propulsion were to give the fifth stage a horizontal velocity greater than that required for orbiting at the altitude of burnout (approximately 50 miles) of the fourth stage. The spinning fifth stage would act as a gyroscope and, therefore, maintain a fixed orientation in inertial space while coasting around to approximately the antipodal point; at this point the fifth-stage motor, oriented properly with the velocity vector, was to be fired, placing the payload into desired orbit.

Figure 3 is a photograph of a complete vehicle assembly. Figure 4 shows the vehicle being mounted on the launching aircraft, and Figure 5 is a photograph of the vehicle during the first stage of flight.

During the development of the satellite-vehicle system, numerous facilities and skills available at the Naval Ordnance Test Station (NOTS) were brought to bear on the program. Practically all components were designed, fabricated, and tested in the research and development laboratories and the engineering shops. Figures 6 through 10 show a number of the hardware components of the propulsion system.

Figure 6 is a picture of the metal parts for one of the four motors in the first- and second-stage cluster. This is the HOTROC motor. Figure 7 is a photograph of the third-stage motor, which was procured from the Alleghany Ballistic Laboratory. This motor, designated ABL 241, uses a cast propellant charge. Figure 8 is a photograph of the fourth-stage 8.0-inch motor and the payload into which is mounted the fifth-stage retro rocket. Figure 9 shows the machining operation developed for processing the 8.0-inch extruded propellant charge for this motor. The propellant is JPN. Figure 10 is a photograph of the fifth-stage 3.0-inch-diameter retro rocket. This motor employs extruded double-base X-14 propellant, which is subsequently machined to

[redacted]

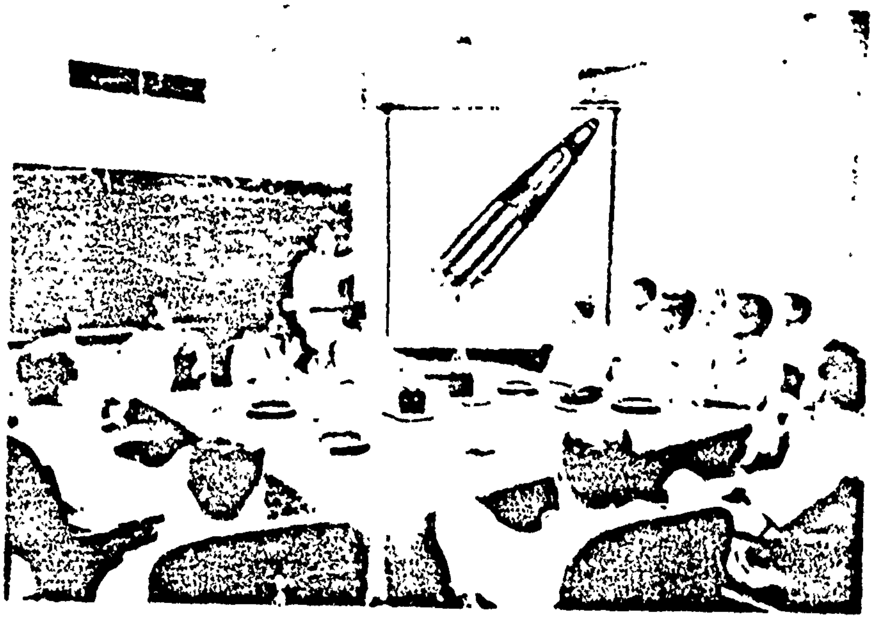

Figure 1 Air-launched satellite and Argus project team.

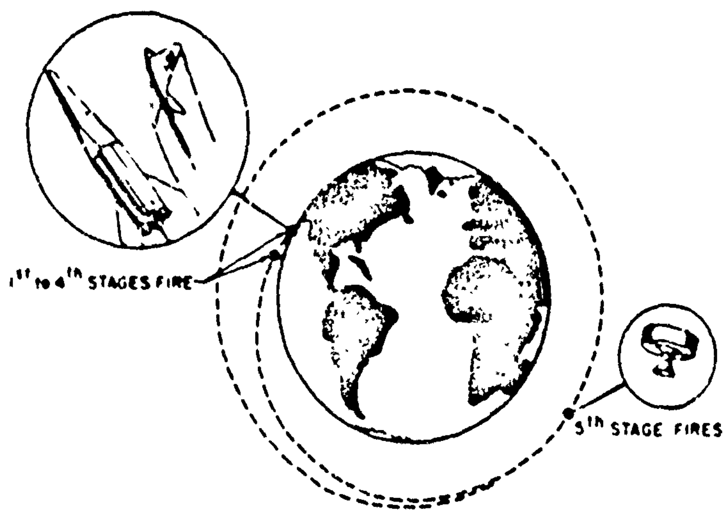

Figure 2 Air-launched vehicle concept.

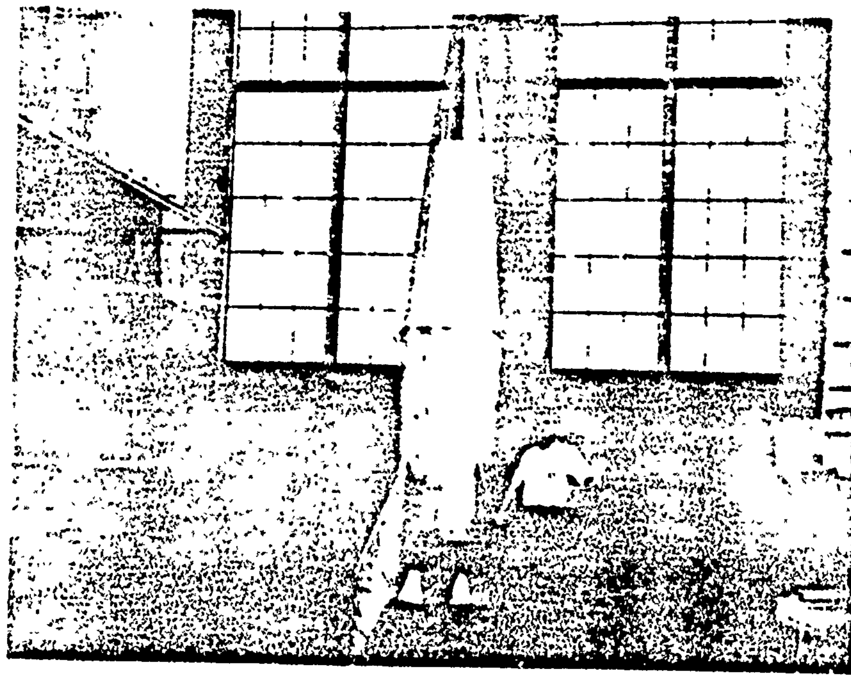

Figure 3 Air-launched vehicle.

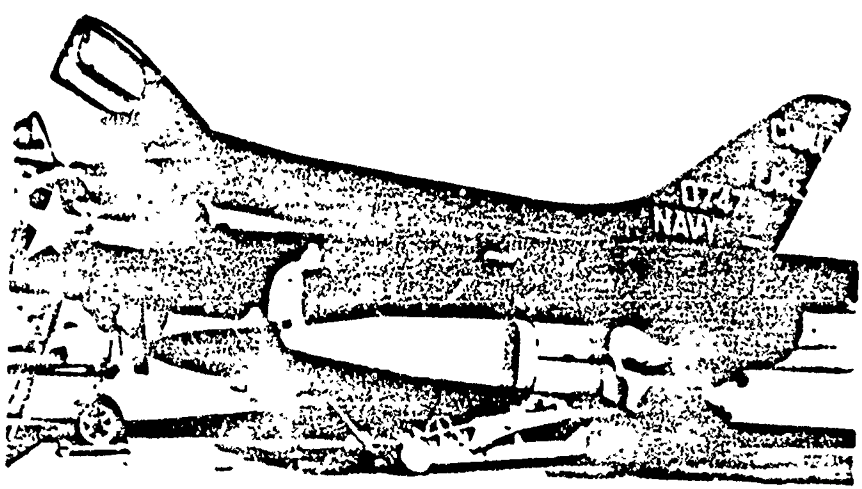

Figure 4 Loading vehicle in aircraft.

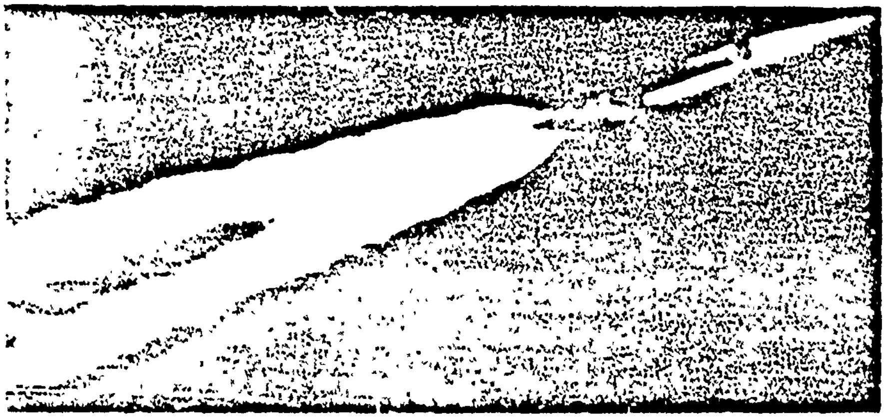

Figure 5 First-stage flight of vehicle.

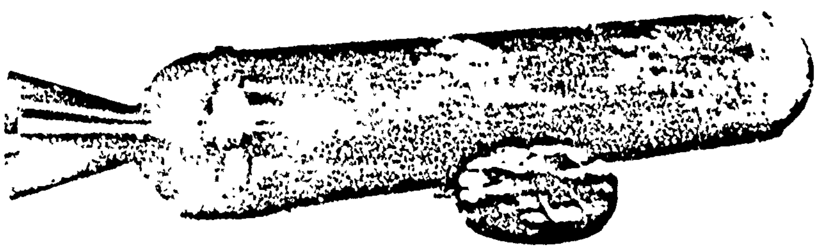

Figure 6 HOTROC first-stage motor.

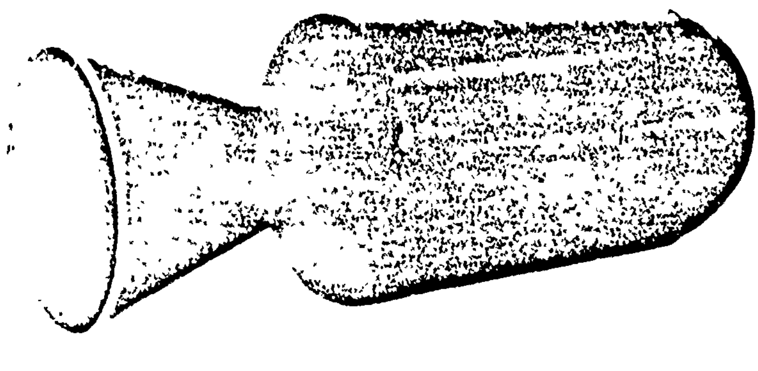

Figure 7 Third-stage motor (ABL 241).

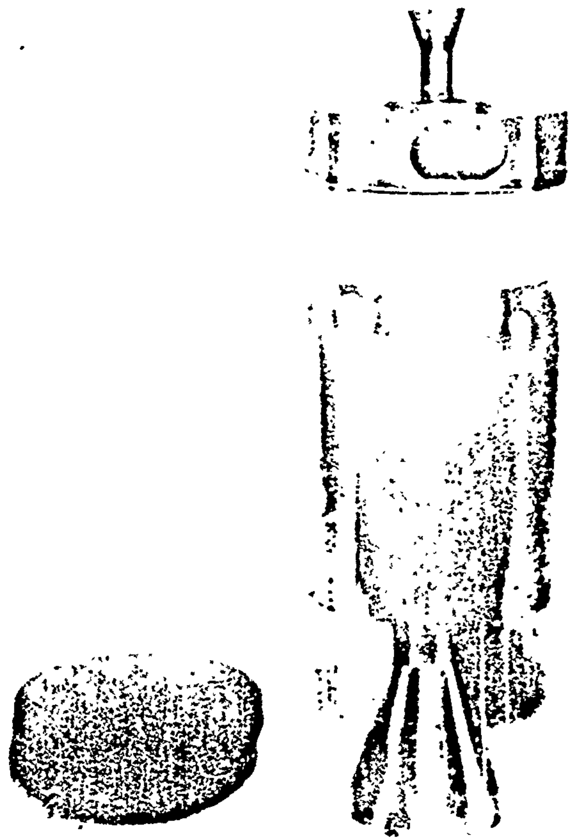

Figure 8 Fourth- and fifth-stage motor with satellite payload.

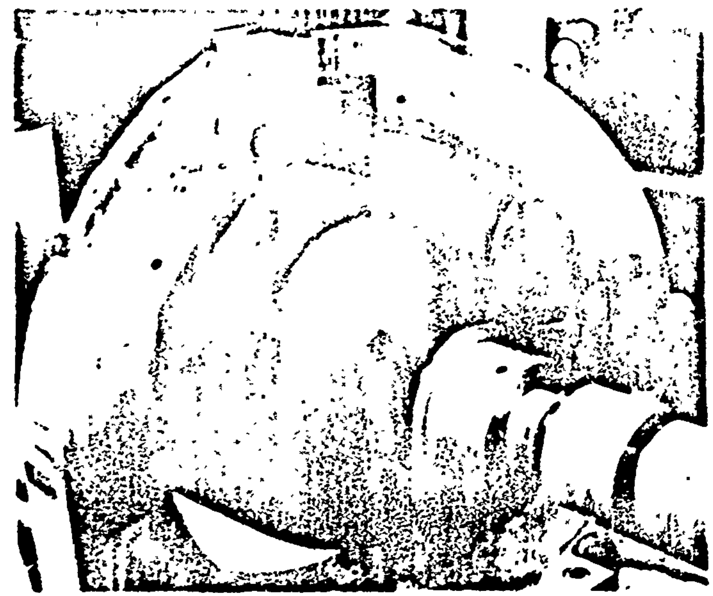

Figure 9 Propellant machining 8.0-inch extruded charge.

TABLE 1 PHYSICAL CHARACTERISTICS OF STAGES 1 THROUGH 5 OF THE VEHICLES

Item	Weight	Initial Stage Weight	Burnt Stage Weight	Stage Total Impulse	Burning Time	Thrust	Nozzle Exit Area	Specific Impulse lb-sec/lb
	lb	lb	lb	lb-sec	sec	lb	in²	
1st Stage:								
Motor metal parts	142							
Propellant	645	2,156.09	1,311.09	140,500	3.47	40,490	145	218 sea level
	787							
2nd Stage:								
Motor metal parts	142							
Propellant	645							
Fins, structure, fairing, timer	100	1,511.09	664.09	140,500	3.47	40,490	157	218 sea level
	887							
3rd Stage:								
Motor metal parts	56							
Propellant	377							
Fairing	10	482.09	105.09	98,058	28	2,724	Vac	260.1 (Alt)
	443.0							
4th Stage:								
Motor metal parts	6.9							
Propellant	27.5							
Fairing and timer	1.24	39.09	11.59	7,020	5	1,404	Vac	255 (Alt)
	35.64							
5th Stage:								
Payload	2.2							
Motor metal parts	0.5							
Propellant	0.75	3.45	2.70	174	1	174	Vac	232 (Alt)
	3.45							

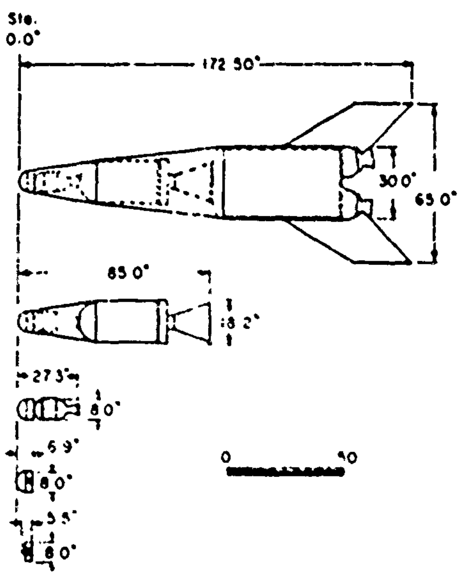

CONFIDENTIAL

a spherical shape to mate with the motor chamber. Figure 11 shows the static test facility for the cluster of HOTROC first- and second-stage motors.

GROUND LAUNCHING OF STRUCTURAL TEST VEHICLES

Four structural test vehicles were ground launched from the NOTS G-2 range to evaluate the integrity of the vehicle design. Two of these vehicles were instrumented with land-line telemetering equipment. Figure 12 shows the vehicle on the ground launcher. Prior to the assembly of the rounds for ground-launching tests, static-load tests were made on components of the airframe. Figure 13 shows the static-load test set-up for evaluating the bird-cage section of the airframe.

All ground-launching tests were made in July and August of 1958. These tests employed live first-stage motors. In the first test, camera records showed that one of the first-stage HOTROC motors ruptured 0.7 second after launch. Examination of the missile after firing indicated a ruptured motor case, which was attributed to a marginal design or cracked propellant charge. Two additional structural test vehicles were launched on 16 and 17 August. Ground-camera records showed that both vehicles failed at approximately 3 seconds after launch near the end of burning of the first-stage motors. These were believed to be propulsion failures. The stabilizing fins also failed to withstand the air loads imposed by firing the round on the ground; however, this problem would not be present in the normal aircraft launching of the missile.

In the final ground-firing test, the first-stage motor blew up on the launcher at ignition. It is believed that a faulty propellant charge was the cause of this failure.

Since all four attempts at ground launchings were unsuccessful and attributable to first-stage propulsion problems, every effort was made to increase the quality control in the manufacture of the propellant charges. The design of the propulsion system was known to be marginal, but time was running out to meet the deadline; hence, it was necessary to settle for quality control measures in lieu of a redesign of the first-stage propulsion unit.

AIRFRAME DEVELOPMENT AND AIRCRAFT COMPATIBILITY

Aerodynamics. The specifications for the external geometry of the vehicle were determined after wind-tunnel tests and a series of scale-model firings in the Aeroballistics Laboratory. Figure 14 shows the scale models for these tests along with the sabots for use in firing the models from a 3-inch gun.

The static aerodynamic stability and dynamic stability of all the rigid-body modes of motion were investigated. A quasi-steady analysis of the stability of the vehicle and its various stages was worked out and stability criteria established. Figure 15 reveals the airframe structure or bird-cage portion of the vehicle.

A complete six-degrees-of-freedom simulation and program has been mechanized for the IBM 704, making it possible to examine stability concurrently with the determination of orbital trajectories.

Studies of the aerodynamic coefficients of the final vehicle were made at the Naval Ordnance Laboratory, White Oak, Maryland. This data was used by the Naval Proving Ground, Dahlgren, to make a complete study of the missile performance utilizing the Naval Ordnance Research Development Center computer facility.

Aerodynamic Heating. Aerodynamic heating was studied with a radiant-heat facility to determine the ability of the nose cone, payload, and first-stage stabilizing fins, including most of the external structure of the vehicle, to stand the predicted environment.

Load Criteria. Loads on the vehicle were examined both as an airborne store and as a free-flight vehicle.

The fin structure was tested for strength and flutter over a limited range of conditions by full-scale tests on the NOTS Baker-4 track. Figure 16 shows the vehicle on the track awaiting the fin test.

Figure 10 Fifth-stage retro-rocket motor.

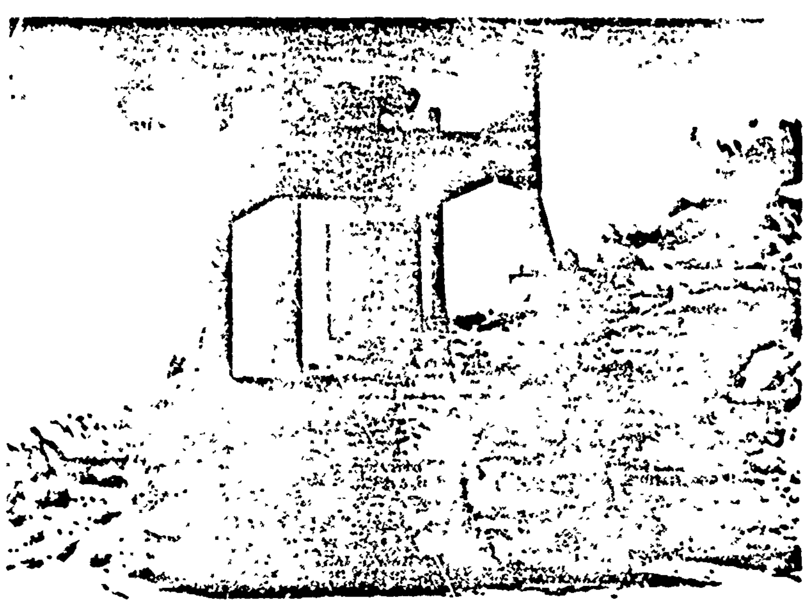

Figure 11 Static testing of first- and second-stage motor cluster.

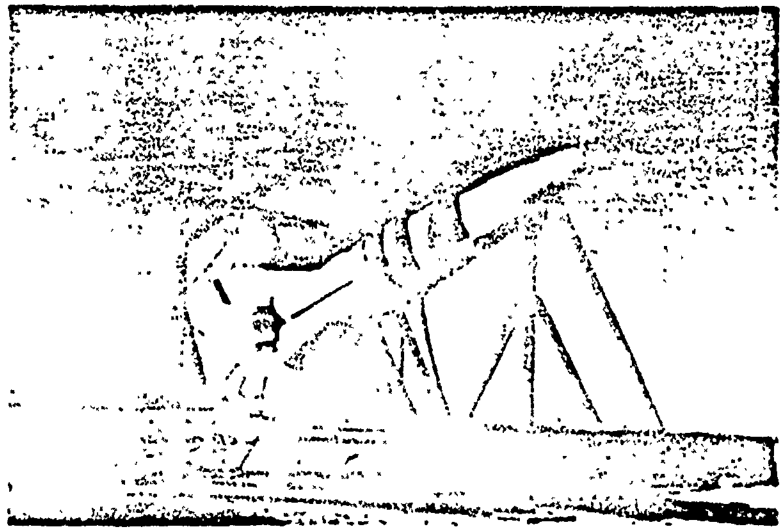

Figure 12 Satellite vehicle on ground launcher with land-line telemetering equipment.

Figure 13 Static-load testing of airframe structure.

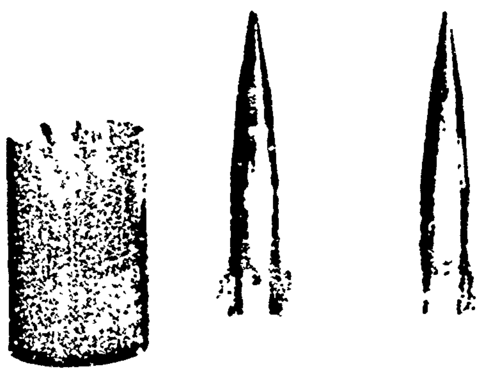

Figure 14 Aeroballistic Laboratory models, $^1/_{15}$ scale.

Figure 15 Satellite vehicle airframe structure.

Aircraft Compatibility and Launching. A compatible installation of the vehicle on the F4D-1 aircraft was achieved. The aircraft performance was investigated relative to the determination of the optimum pull-up trajectory for launching by the Douglas Aircraft Company (DAC). Also a limited wind-tunnel program was conducted with DAC to investigate the release, launch, and separation of the vehicle from the aircraft.

Instrumented dummy stores were flown on the aircraft to determine aircraft and missile loads during all phases of the airborne flight from takeoff to missile release. Also, after the LABS gear was calibrated, the maneuver was practiced for consistency without dropping the

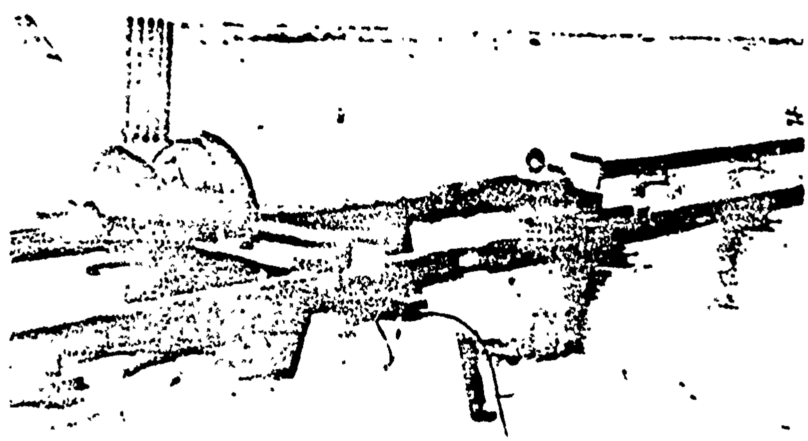

Figure 16 Vehicle flutter-fin test on B-4 track.

store. On each run, internal aircraft instrumentation as well as external camera coverage recorded the aircraft performance.

Four preliminary test flights were made to determine if the F4D aircraft could perform the required maneuver for launching the satellite vehicle. It was learned that the 59-degree pull-up could be achieved. Two flights were then successfully made at a 58-degree pull-up as an aero-ballistic shape simulating the vehicle was dropped.

Instrumentation of the six attempted launchings for orbit revealed the following results:

Desired Launch	Average for Six Firings	Minimum	Maximum
Speed, 700 ft sec	689	670	750
Angle of launch, 59 deg	58	57	60
Altitude, 35,000 ft	37,250	36,800	37,500

Table 2 is a summary of the preliminary tests carried out to evaluate the vehicle design.

Figure 17 shows a complete vehicle structure receiving final inspection in the engineering shop prior to being loaded for subsequent evaluation.

SCINTILLATION COUNTER PAYLOAD

The purpose of the scintillation counter was to measure beta radiation in a polar-orbiting satellite in conjunction with the Argus experiments

Operational specifications and circuitry for the instrumentation were provided by James Van Allen, of the State University of Iowa. Physical design and construction, systems compatibility studies, testing, and calibration were accomplished by personnel of NOTS.

The completed payload was to measure beta radiation that exceeded 1.5 Mev energy level, with the information telemetered back to earth via an FM-FM system, modulated by the output

TABLE 2 SUMMARY OF NOTS PROJECT FIELD TEST WORK

Tests conducted at China Lake, California. STV: Structural Test Vehicle.

Date	Round No.	Range	Type of Test	Number of Instruments	Processing*
1958					
9 Jun	1	G-1	F4D Aircraft 20° pull-up	22	24 hr
11 Jun	2	G-1	F4D Aircraft 55° pull-up and drop	22	No data
13 Jun	3	G-1	F4D Aircraft 55° pull-up and drop	22	36 hr
13 Jun	4	G-1	F4D Aircraft 55° pull-up and drop	22	36 hr
6 Jun	1	G-1	Ground launch horizon scanner	9	2 wk
13 Jun	2	G-1	Ground launch horizon scanner	9	2 wk
28 Jun	3	G-1	Ground launch horizon scanner	9	2 wk
[illegible] Jul	4	G-1	Ground launch horizon scanner	9	2 wk
19 Jul	1	G-1	F4D Aircraft 58° pull-up, no drop	22	1 wk
19 Jul	2	G-1	F4D Aircraft 58° pull-up, no drop	22	1 wk
19 Jul	3	G-1	F4D Aircraft 58° pull-up, no drop	22	24 hr
23 Jul	4	G-1	F4D Aircraft 58° pull-up, no drop	22	1 wk
23 Jul	5	G-1	F4D Aircraft 58° pull-up and drop	22	24 hr
23 Jul	6	G-1	F4D Aircraft 58° pull-up, no drop	22	1 wk
23 Jul	7	G-1	F4D Aircraft 58° pull-up and drop	22	24 hr
18 Jul	1	G-1	Horizon scanner launched from F3D Aircraft	9	2 wk
20 Jul	2	G-1	Horizon scanner launched from F3D Aircraft	9	—
20 Aug	1	G-1	Preliminary launch of STV from F4D Aircraft	27	24 hr
4 Jul	1	G-2	Ground launch STV	50	8 hr
20 Jul	1	G-2	Ground launch STV	51	No coverage
16 Aug	1	G-2	Ground launch STV	54	24 hr
17 Aug	2	G-2	Ground launch STV	54	24 hr
	4	B-4	Fin-Flutter Test	—	—
6 Jun	1	B-4	Acceleration	3	No processing
15 Aug	—	—	Dress Rehearsal	54	None

*Time required after firing for data processing

of two scalers, which were scaling 64 and 4,096 times. The payload was to have a minimum radiated power of 25 mw, nominally, operating at 108.00 Mc, and with an expected life of 2 weeks. Two standard subcarriers of 960 and 1,300 cycles median frequency were specified. Figure 18 shows a complete payload package. Figures 19 through 22 show components of the payload. Figure 23 shows the timer for the two last-stage motors being assembled in the nose of the vehicle.

A severe maximum weight limitation of 2.3 pounds for the complete package presented several difficult problems in design and miniaturization to be solved by the personnel of NOTS. A weight table for a completed payload is given in Table 3.

The payload development included design of a miniaturized RF transmitter using only transistors, transformerless subcarrier generators using a temperature stabilized R-C type of frequency control system, and transformerless FM modulating system for the RF transmitter.

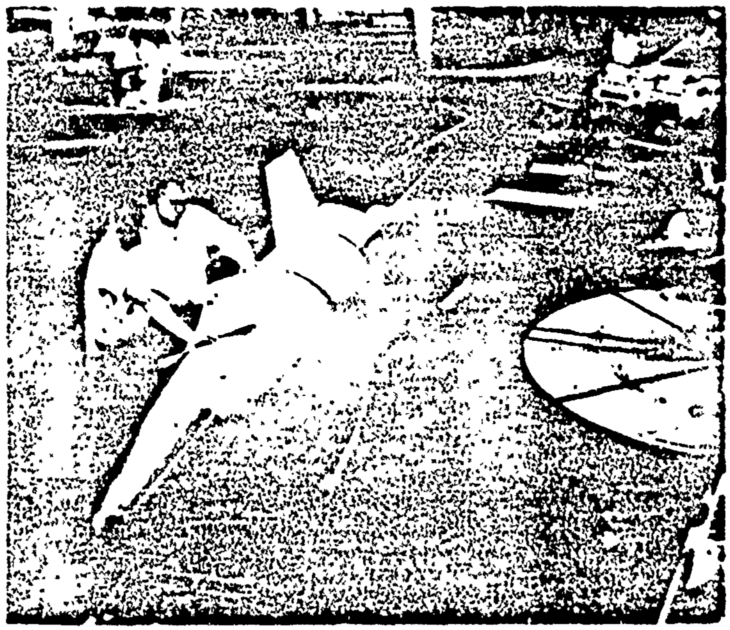

Figure 17 Final inspection of vehicle.

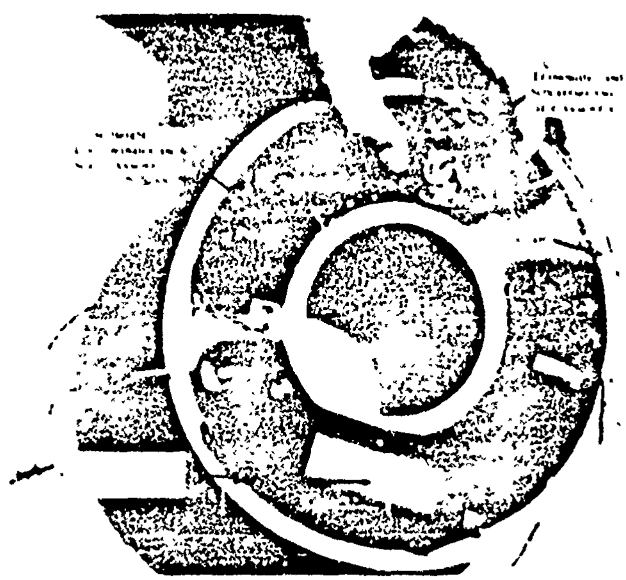

Figure 18 Complete payload package. (This view does not show all batteries, or turnstile antenna.)

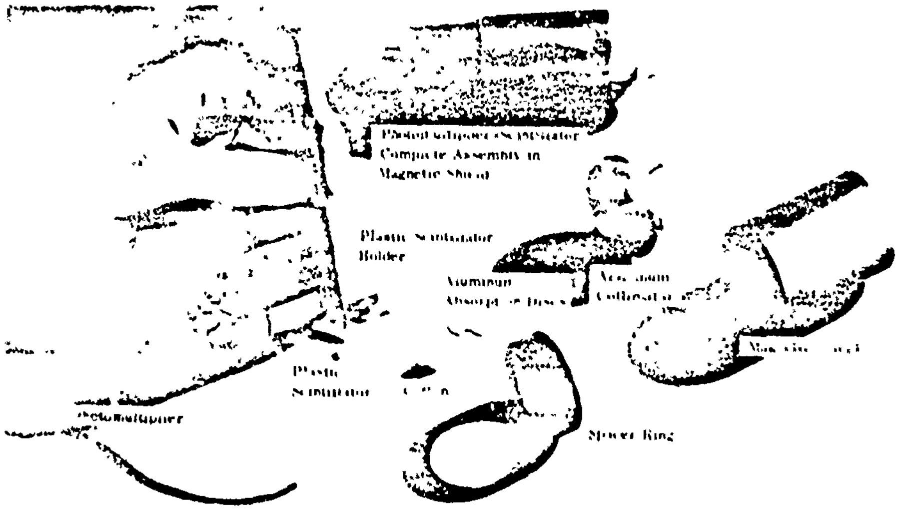

Figure 19 Photomultiplier-scintillator components.

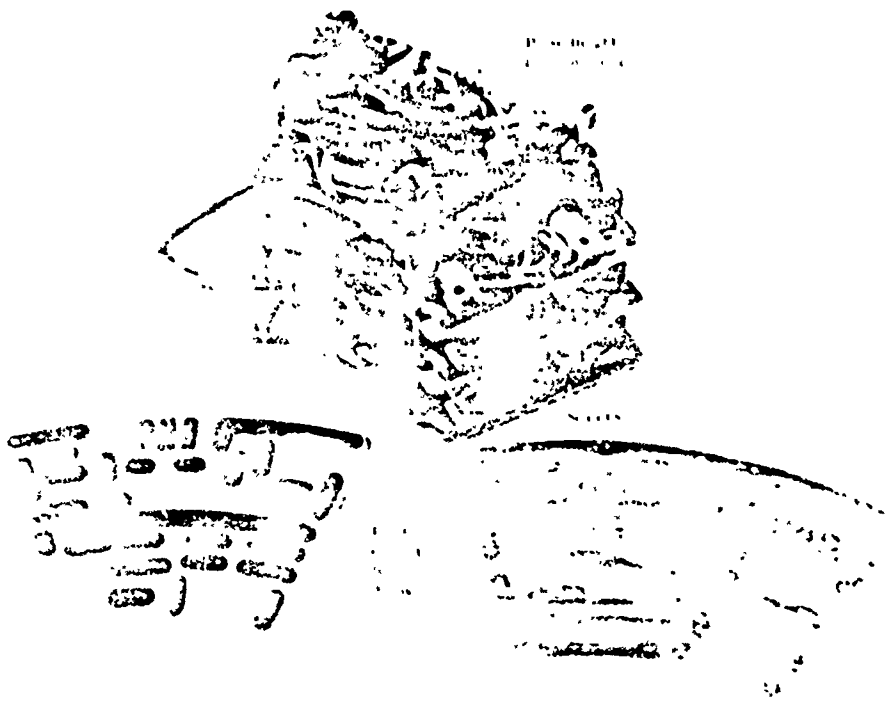

Figure 20 Pulse-height discriminator and scalers.

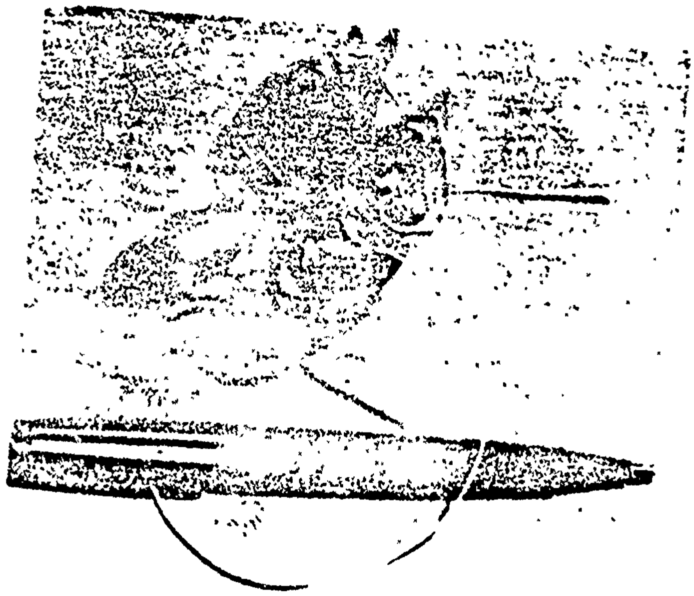

Figure 21 Power-supply inverter.

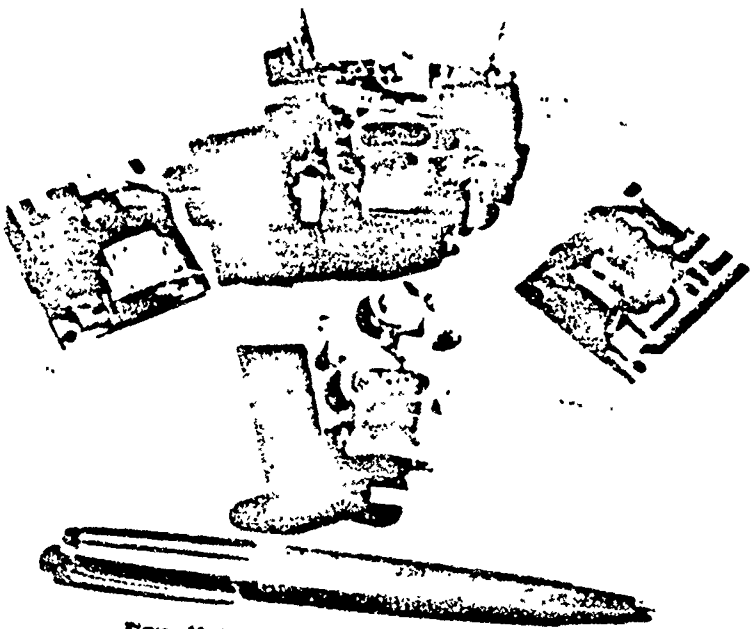

Figure 22 Transmitter and subcarrier oscillators.

These included a mixing preamplifier for adjustment of the modulation indices, with all modulating circuits operating from the same batteries as the RF transmitter.

Another difficult problem in design was the antenna system. It had two modes of operation: an interim mode, in which RF radiation was to be provided by a modified dipole, and the primary mode, provided by means of a turnstile antenna. The turnstile was for omnidirectional

Figure 23 Fourth- and fifth-stage timer being assembled in nose of vehicle.

radiation after separation of the payload from the missile. The interim mode was to be used for tracking purposes while the vehicle was borne by the launching plane and during two phases of rocket propulsion.

Instrumentation. The scintillation counter consisted of a plastic scintillator cemented to the face of a Type 6199 photomultiplier tube, with a pure-aluminum absorber to limit the measurements to sufficiently high energy levels and a special aluminum collimator (see Figure 19). It also had a pulse-height discriminator to set the energy level for counting at 1.5 Mev or above, with scaler counters of 64 and 4,096 times and emitter-follower outputs for keying the subcarrier generators.

Included with the instrumentation section was design and construction of a regulated high-voltage source, utilizing a transistor inverter system (see Figure 24).

Transmitter. The transmitter operated at 108.00 Mc nominally, with the frequency controlled to close tolerance by means of a third-overtone crystal. The oscillator, utilizing a Type 2N500 transistor, operated at 54.00 Mc, driving a doubler-amplifier that utilized two Type 2N500 transistors in a parallel-grounded base configuration. The FM transmitter delivered 30 mw to the antenna system, the output level being adjusted to the desired amount by proper selection of a bias-resistance, limiting-emitter current in the oscillator. This adjustment was made prior to potting in the completed payload.

Frequency modulation of the transmitter was accomplished by varying the voltage applied to the oscillator, in accordance with the combined subcarrier modulating signal, via the special

TABLE 3 WEIGHT TABLE FOR TYPICAL PAYLOAD

NOTS Project Payload, Type A

Items	Weight in Grams
1. Outer case and cover	128
2. Paint	12
3. Turnstile antenna, cups and covers	13
4. Potting compound	115
5. Batteries (for 288 hour operation)	473
6. High voltage supply (converter)	55
7. Magnetic shield	10
8. Photomultiplier tube (RCA 6199)	67
9. Collimator	19
10. Adapter	4
11. Plastic shield	5
12. Scintillator (plastic)	1
13. Pulse-height discriminator	20
14. Scalers (three circuit boards)	63
15. Transmitter [illegible]	40
	[illegible]

Total weight [illegible] pounds

modulating system. The index of modulation was adjusted by setting the levels of the individual subcarrier signals. Figure 25 is the circuit diagram of the RF transmitter and modulator.

Subcarrier Generators. Because of the weight limitations, it was necessary to develop a new transformerless type of subcarrier generator. The generators were designed to operate in the standard subcarrier channels of 960 and 1,300 cycles median frequency. They were of the FM type, being deviated between ± 5 percent limits by the off-on type signals from the emitter-follower outputs of the scalers.

The subcarrier generators were of new design with a low power requirement, using temperature-stabilized RC frequency control circuits, and were stabilized between + 10 C and + 60 C. The degree of deviation with a given signal, versus temperature, was not linearized. This was not thought to be necessary, because of the nature of the modulation, so long as the frequency did not drift outside of the channel limits. Therefore, some divergence of the excursion limits, with an increase in temperature, was ignored.

Several types of alternate design were tried, but all had serious adverse effects. Since weight limitations did not permit use of iron-core inductances of normal dimensions, an attempt was made to use Dot $\frac{1}{10}$-ounce transformers as inductances, as well as other subminiature devices.

These methods all proved unsatisfactory, as they were highly sensitive to changes in both supply voltage and temperature. Proper deviation of their frequency was difficult; the output wave form was very poor, changing radically with deviation of the frequency and with slight change in supply voltage.

Modulation System. Since no iron-core devices could be used, a modulating circuit for the RF transmitter was designed using a Type 2N206 transistor, operating in a common collector configuration. This modulator varied the voltage applied to the RF oscillator in accordance

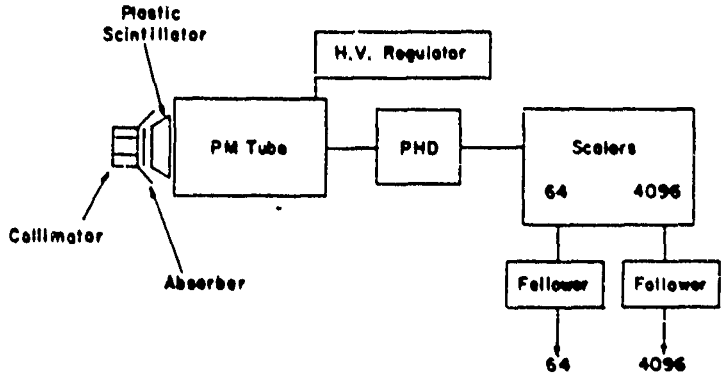

Figure 24 Schematic of the scintillator counter.

with the modulation signal. This circuit had unit voltage gain, thereby applying an identical signal to the oscillator circuit as that of the combined modulation signal. It had a stiff bias circuit to prevent distortion of the modulation signal with temperature rises, with a secondary purpose of bypassing part of the necessary oscillator current around the modulating transistor.

A modulation pre-amp mixer stage was used to enable proper adjustment of modulation levels and proper combining of the two subcarrier signals into a single, complex modulation signal.

Antenna System. A unique system was designed for this application, having good impedance-matching characteristics and radiation efficiency at all times.

In the primary mode of operation, by means of the turnstile configuration, feed to the first elements was accomplished by equal lengths of miniature 50-ohm coaxial transmission line. These elements were spaced opposite each other on the payload, fed by individual coupling coils, 180 electrical degrees apart. The second elements, also opposite each other, but 90 degrees from the first, were fed from the first elements by means of quarter-wave-phasing sections. Each element was fed 90 degrees from its respective first element. This resulted in a quadrature configuration, with each element located physically 90 degrees from any adjacent one and excited 90 degrees from any adjacent one. Field-strength measurements showed the pattern to be nearly a sphere of radiated signal, with the antenna actually radiating.

Radiation in the secondary mode of operation was by means of the modified dipole, located in the nose cone of the missile. This mode was for purposes of tracking during the time that the missile was borne by the launching plane and during firing of the first and second rocket phases of propulsion. Upon firing of the third rocket phase, mode changed to the primary one.

Since no protuberances could be tolerated, the dipole antenna for interim radiation was necessarily installed within the fiberglass nose cone (Figures 26 and 27). It was necessary to extend the elements along the length of the nose cone, the required length of the elements being approximately 26 inches. This fact presented a problem in avoiding cancellation of signal, due to the nearly parallel placement of the elements. This problem was solved by extending the ele-

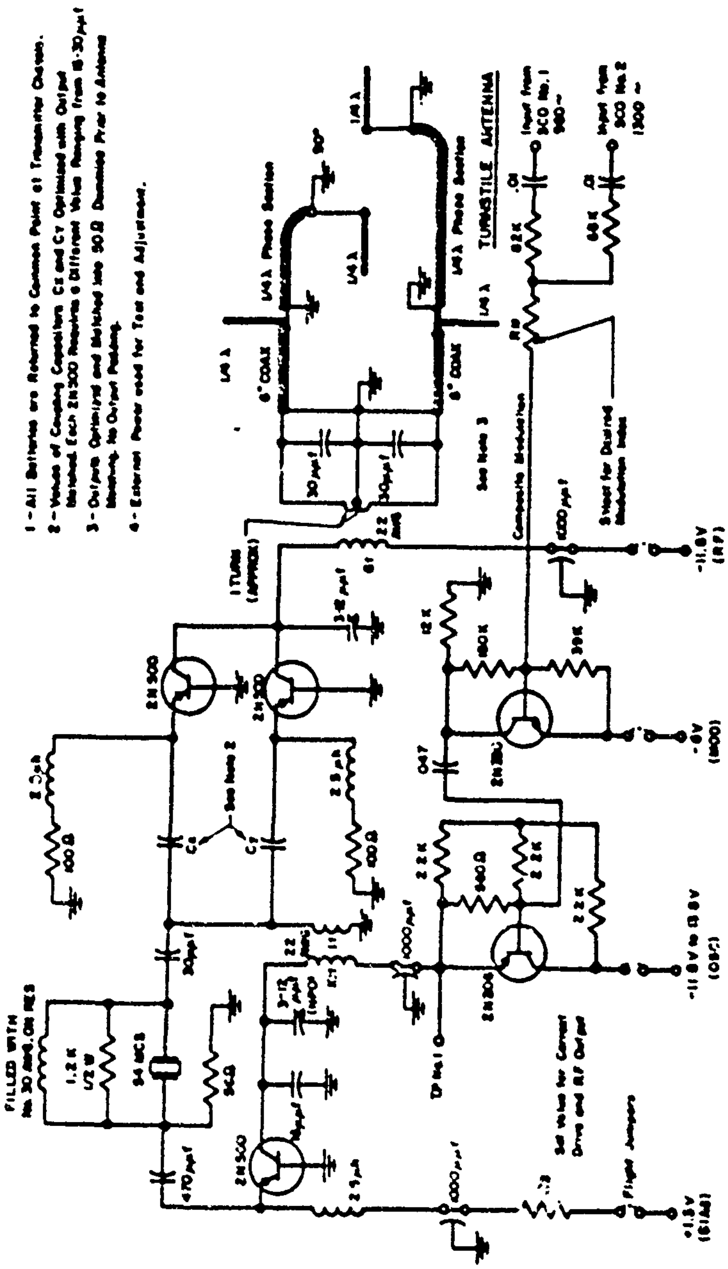

Figure 25 Circuit diagram of the RF transmitter and modulator.

ments only a short distance from the points of signal feed in a parallel manner. Each element was then spiraled at a 45-degree angle with respect to the longitudinal axis of the nose cone. This can be visualized by imagining one is looking through the nose cone. At some particular point, where the elements are spiraled, they would appear to be at right angles with each other.

This modified dipole was fed 180 electrical degrees apart at the position of the first elements of the turnstile, through coiled and shorted turnstile elements. The second set of elements of the turnstile were also coiled and shorted out.

Good impedance match to the transmitter was obtained during both modes of operation, with excellent loading. Actual field strength pattern measurements were not made of the interim mode of operation, however.

Unique design was employed in providing the requisites for both modes of operation. It was necessary to provide: (1) turnstile configuration for the primary mode of operation; (2) dipole configuration during interim operation; (3) retaining cups in the payload skin for carrying the turnstile elements during dipole operation, with connection anchors at the center point of the payload sidewall, in each case; (4) antenna cup covers, upon which the coiled turnstile elements are supported until such time as they are required to be extended for use; (5) a means of shorting out each turnstile element, during dipole operation, to prevent interaction with the transmitter, due to inductance changes resulting from vibration and shock; (6) a means of feeding RF to the modified dipole antenna during interim operation, from the disabled turnstile elements; and (7) a sure means of forcing payout of the turnstile elements, at such time as they are required, in such a manner that they would not tangle during their extending.

Antenna cups, approximately ¼-inch deep and 1 inch in diameter were secured into holes in the sidewall of the payload, with connecting anchors located at the center point of the can sidewall and bottom of each cup. These were for connection of each feed line internally and each turnstile element externally (see Figure 28).

Covers for each cup were used, upon which were supported the coiled turnstile elements. Through each cover was a stranded wire, for external connection to the dipole elements at two positions, and two jerk wires at the other positions. Internally, the stranded wire was [illegible] and trimmed to three strands, two strands being connected directly to the balled outer end of each turnstile element. This was to pull the end of the wire outward at such time as the cover was pulled away. At time of assembly, the single strand was connected,together with the turnstile element, into the connecting anchor. This yoke provided the means of forcing payout of the turnstile element as the cover was ripped away at separation of the payload from the missile. It also provided the necessary shorting of the coiled turnstile element during dipole operation.

The sequence of doing this was as follows: Each cover was overlaid on the inner surface with a "tacky wax", upon which was spiraled the turnstile element, starting at the outer edge and coiling toward the center. The turnstile elements were of gold-plated, annealed, braided copper wire. After spiraling of the element, a sort of retaining basket was fashioned by use of a single strand of wire around the cover crossing the spiraled element in each direction. The wax was next dissolved out by means of a degreaser, and the connection yoke installed (see Figure 29).

Upon assembly of the payload in the missile, the previously prepared antenna element was installed in each cup, first placing a small plug of fiberglass wool within the cup. This was to bear against the coiled antenna element to hold the spiral in place, after removal of the fine strand basket. The basket was removed at the time of assembly. The cover was then held in place by a piece of tape only until the payload was secure in the nose cone of the missile.

After partial insertion of the payload into the nose cone, connection was made to the elements of the modified dipole and the two jerk wires. At each of these points, the nose cone had been prepared with a larger piece of fiberglass wool, which folded double as the payload was inserted. This provided considerable pressure against each cup cover to hold it in place until separation from the missile.

Therefore, as the payload moved out of the nose cone, the interim dipole elements and the jerk wires would lift away the cover from each antenna cup. The double strand in each yoke would start to pull the free end of each element out of the cup. Simultaneously, the single strand

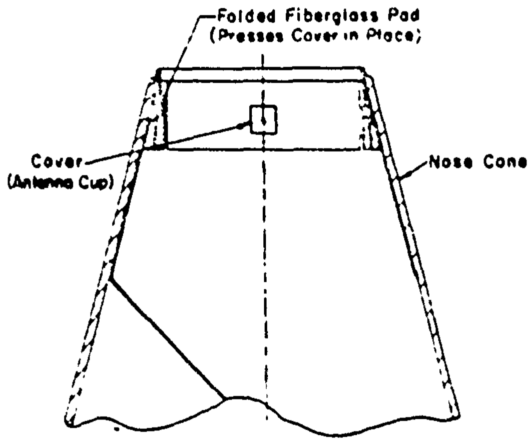

Figure 26 Cross-sectional view of nose cone and payload.

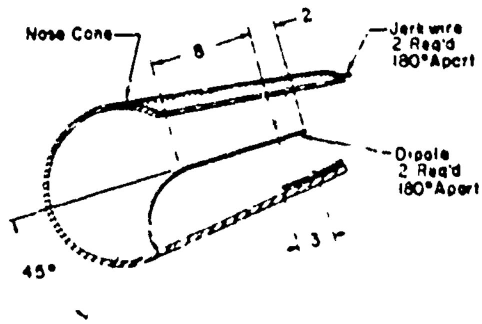

Figure 27 End view of nose cone and payload.

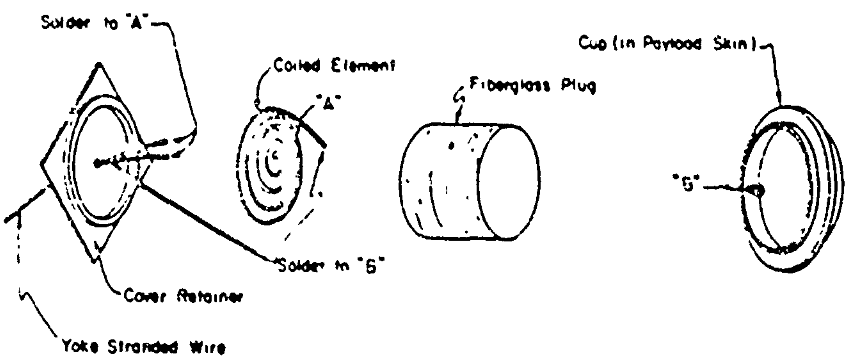

Figure 28 Antenna-element assembly

of the yoke would break at the connecting anchor, removing the short from the turnstile element. Extending of each element would continue, whether or not the yoke broke away from the end of the element, due to centrifugal force (rotation is 5 cps). The dual strand of the yoke would rip away from the end of each element, in any event, at the end of payout.

Weight Limitations. In the entire payload, components were given special attention regarding their ruggedness and temperature stability, and the lightest type was selected where there was a choice. Subassemblies were of printed-circuit design to enable reduction of weight with-

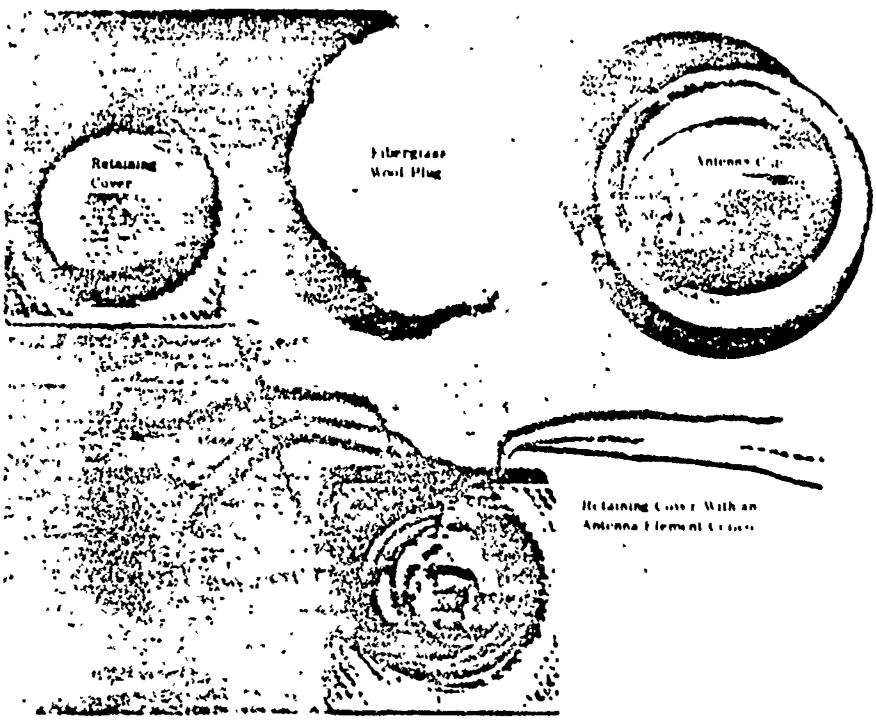

Figure 29 Antenna elements.

out sacrificing dependability wherever possible. The RF transmitter was made on a chassis of brass shim stock, appropriately crimped and stiffened to make an extremely light assembly, using air-core coils stiffened with epoxy resin.

The subcarrier generator boards were mounted on each side of the RF transmitter, effectively shielding the uncoupled radiation of the transmitter, without extra shielding. This resulted in a complete transmitter, subcarrier and modulator assembly weighing only 43 grams.

Packaging. The completed payload was in the form of a doughnut, $7\frac{1}{4}$ inches in diameter and $2\frac{1}{2}$ inches high, with a 3-inch center hub, into which was installed the rocket motor for the final phase of propulsion.

Rigidity for the entire assembly was afforded by use of a foam potting compound. This was used for prevention of adverse effects from vibration, shock, and accelerations. After installation of the coaxial transmission lines and antenna retaining cups, flight jumper terminal board and feed-through insulators, the entire container was given a preliminary potting. This was heat-cured for added strength. The compound was then channeled out to permit installation of the various subassemblies and batteries, illustrated in Figure 30.

The subassemblies and batteries were carefully placed in the channel, so as to give good approximation of balance. Connections were then made to all components. All items were placed

Figure 30 Payload case and antenna.

with their gravity centers at the midpoint of the channel, as nearly as possible, for good dynamic balance. Good balance was then accomplished by use of a ball-bearing gimbal mounted in the hub, supported from the ceiling by a string. Compensations were then made and the final potting done. Balance was then again trimmed by slight cutting away of potting material or inserting small copper wire at the periphery of the package, when necessary.

Source of Power. A most important consideration was the power source. From the start, it was borne in mind that the project could be successful only if design was in such a manner that the various subassemblies and devices required low power consumptions. Excessive power requirements precluded the use of commercially available assemblies. Mercury batteries were chosen for their good characteristics under changes in temperature, ability to operate in vacuum and for their acceptable power-versus-weight characteristics. Their dimensions and configuration also were good, so that packaging was less difficult.

Other Considerations. Printed-circuit flight jumper boards were installed in the skin of the payload so that external power sources could be used for all testing and adjustment, leaving the internal power sources for actual payload use. This permitted actuation of the payload at the last moments before takeoff.

It was necessary that the payload provide battery power for operation of a squib firing timer assembly and that squib leads be carried through the payload. This was accomplished by using common batteries for the high voltage inverter internally and the timer inverter externally. Connections were made via feed-through insulators installed in the package skin.

It was necessary to provide a means of increasing RF radiation at an elevation sufficiently high for final check with the microlock station, just prior to takeoff of the launching plane. This was accomplished by shock exciting a dipole, elevated on a pole, by taping a short section of each end of the transmission line directly over the interim dipole radiator.

It was found that RF radiation near the scintillator or photomultiplier caused a change in count when a voltage was permitted to develop in that proximity. This was overcome by locating one of the secondary turnstile elements approximately midpoint of the complete scintillation assembly. With the current node and voltage null located in this manner, no adverse effect was caused.

Another important consideration was the returning of all battery sources to a common point at the RF transmitter. By permitting no sources of common coupling, spurious effects were not produced.

At the time of assembly, a piece of cotton was purposely contaminated with a radioactive isotope (P^{32}; half life 14.3 days) and placed in the collimator of the scintillation counter for the purpose of providing a standardizing background count. Continued correct operation of the payload was determined in this manner. This method also served to calibrate and adjust the pulse-height discriminator to the correct energy level of 1.5 Mev.

Tracking. That this system operated efficiently was attested by the fact that the NOTS microlock station was able to track the missile on the aircraft from takeoff until missile launch, at which time function was terminated due to missile failure. This was at a distance of approximately 150 miles with the missile going approximately 5 degrees below line of sight, due to intervening mountain ranges.

PROGRAMMING SYSTEM

One of the most-critical components in the system is believed to have been the horizon trigger. It was a telescope with a narrow field of view, and had an infrared sensitive cell at its focus. Its optical axis was at a 12-degree angle with the vehicle axis. Figure 31 shows the horizon scanner being installed in the vehicle. When the spinning vehicle, with its spent first- and second-stage motors, achieved an attitude of 3 degrees with respect to the local horizontal, IR radiation from the earth's surface was detected by the IR cell. The cell generated a pulse, which was amplified by transistor circuitry until it saturated the output transistor. The saturated output pulse was integrated such that the second-stage motor was to be fired when the earth's horizon had been scanned for at least four times. The purpose of the horizon trigger was to determine the all-important vehicle attitude at perigee so that the second- and third-stage velocity vectors would be added in the correct direction. The horizon trigger would offer a means of nullifying errors in initial trajectory resulting from first-stage mass asymmetries, thrust malalignment, and deviation in aircraft azimuth and vehicle release angle.

Before the first-stage booster was fired, a safe separation distance of about 500 feet between aircraft and vehicle was assured with a 5-second delay timer. As previously explained, the second-stage booster was fired at the end of a coast period by action of the horizon trigger. The firing system provided an enabling timer to prevent premature operation of the horizon trigger from the sun or other sources of IR energy. Fourth- and fifth-stage boosters and the explosive charge to separate these stages were to be fired by additional electronic timers.

HORIZON-SCANNER TESTS

Four horizon-scanner ground launchings were made from the X-8 launcher to determine the performance of this component. Test conditions called for launching the scanner on an HPAG rocket motor at an angle of 55 degrees above the horizon. This angle allowed the scanner to go above the horizon and come to a parallel position relative to the ground at which time it was supposed to fire a spotting charge indicating proper functioning of the scanner.

Figure 32 shows the scanner test vehicle on the ground launcher prior to firing. The test results from these firings and two aircraft firings were not conclusive. In these tests, the

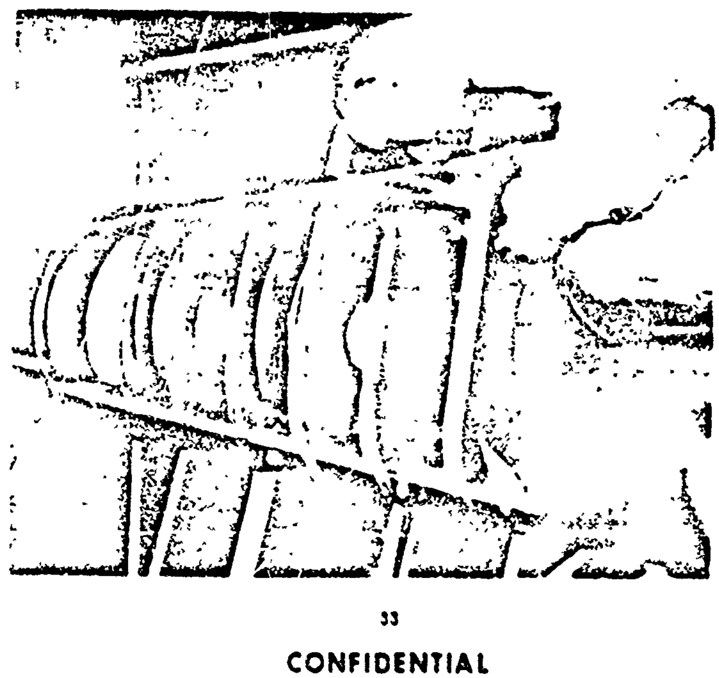

Figure 31 Horizon scanner in vehicle assembly

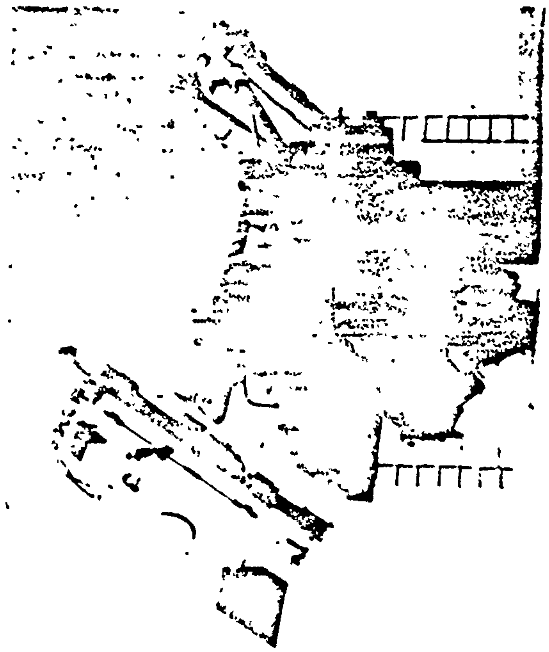

Figure 32 Scanner test vehicle on ground launcher.

CONFIDENTIAL

premature triggering of the horizon telescope by sun glints indicated the need for an enabling timer to gate the period of operation.

GROUND RECEIVING STATIONS

Work on receiving stations was initiated with the Explorer satellite program. A microlock station was built at NOTS and operated in connection with a number of the early satellite programs. The unique feature of the NOTS stations is their improved capability for rapid frequency scan. For Operation Argus, four additional portable stations were operated to record doppler

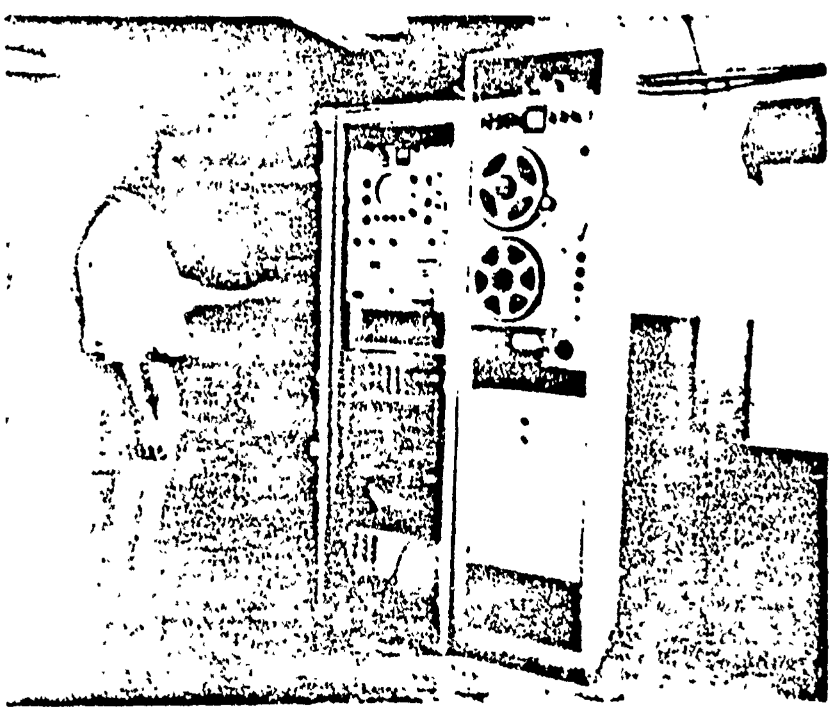

Figure 33 Microlock ground-receiver station.

and telemetering data from Explorer IV. Figure 33 shows a typical microlock ground receiver station. Units with their regulated power supply were air-freighted by MATS to New Zealand, Alaska, Greenland, the Azores, and Hawaii, where they were operated by NOTS personnel. Figure 34 is a map showing world-wide coverage and locations of ground receiver stations. Figure 35 shows a packaged station arriving in New Zealand, and Figures 36 and 37 show the station sites in Alaska and New Zealand. Data from 350 passes of Explorer IV were sent to Van Allen at the University of Iowa. These stations have consistently picked up a 10-mw signal (from Vanguard I) at a slant range of 3,000 miles.

The microlock system is designed to recover two types of information, doppler frequency and telemetering. Two techniques, called a tracking filter and a linear detector, are used to increase receiver sensitivity.

The basic problem in receiving low-level signals in the 100-Mc region is detecting them in the presence of galactic noise. The measure of how well the problem is being solved is called

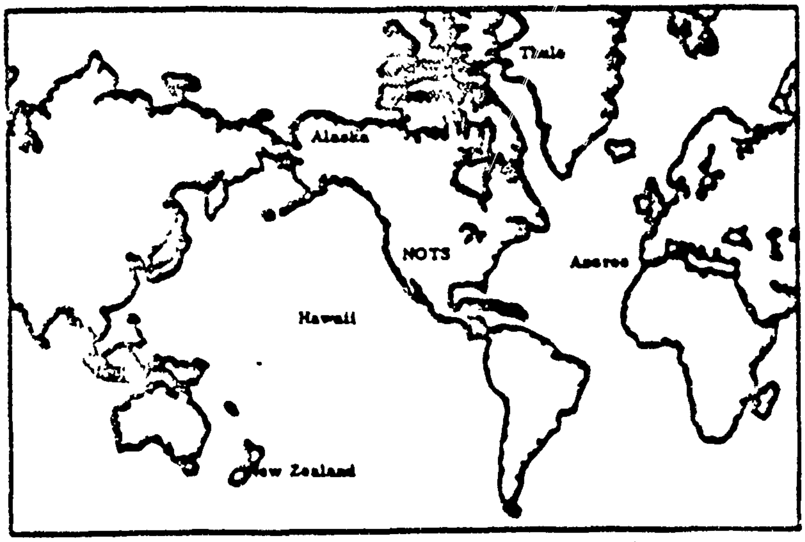

Figure 34 Locations of microlock ground-receiver stations.

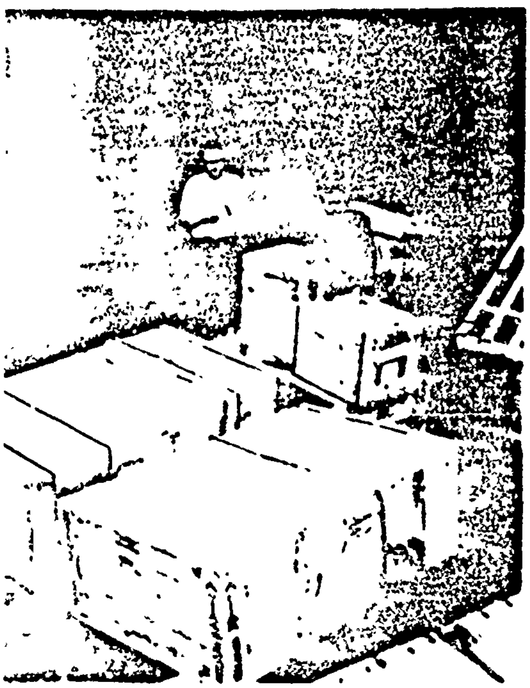
Figure 35 Microlock station equipment in shipping packages.

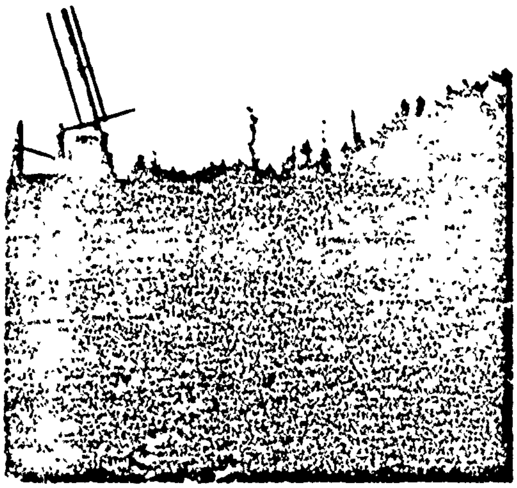

Figure 36 Microlock site in Alaska.

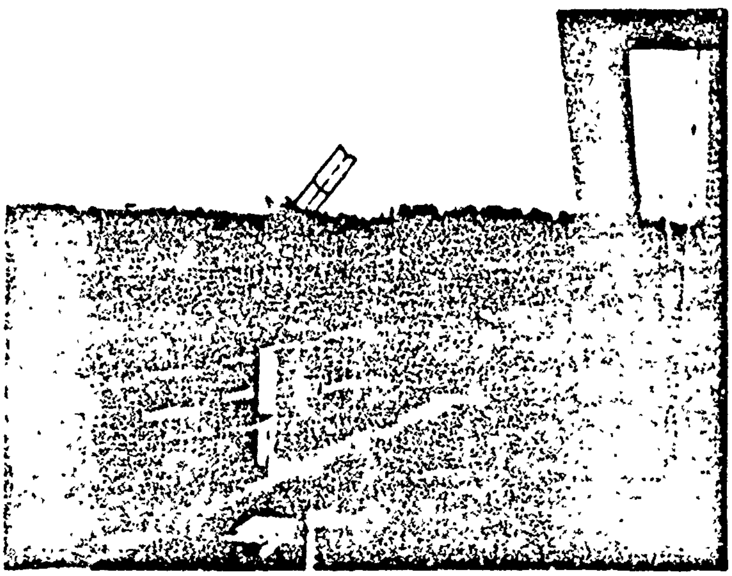

Figure 37 Microlock site in New Zealand.

[redacted]

the signal-to-noise ratio (S/N), where S is the signal power and N is the noise power, the magnitude of which is directly proportional to the required audio bandwidth. The use of the tracking filter as shown in Figure 38 illustrates the principle. The carrier frequency of a satellite, as seen at the receiving station, experiences a shift due to doppler of approximately 8 kc (as

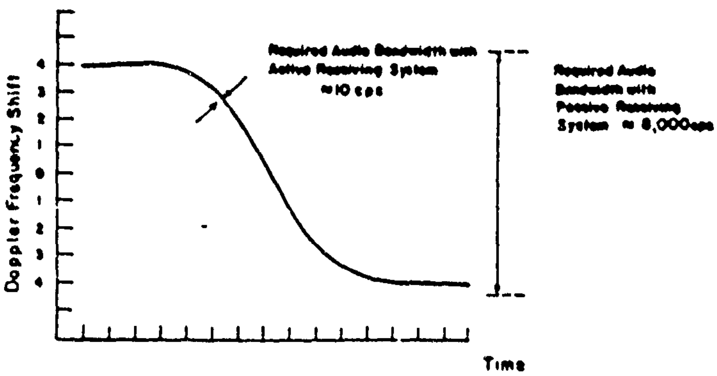

Figure 38 Doppler frequency shift versus time.

determined by receiving station location, orbital parameters, and transmitter frequency). With a passive receiving system, this would require an audio bandwidth of at least 8 kc with a resulting noise power proportional to the 8-kc bandwidth. With an active filter tracking the incoming signal, the bandwidth can be reduced to approximately 10 cycles; hence, there is a tremendous

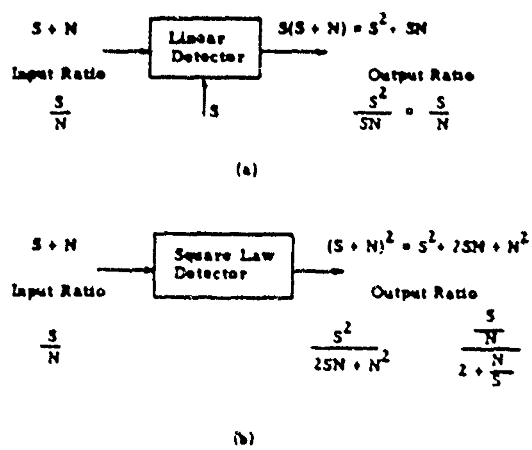

Figure 39 Equations for linear and square-law detection.

reduction in noise power with an equivalent increase in S/N ratio. The increase is obviously proportional to the reduction in bandwidth, or 8,000 to 10.

Linear detection also works to preserve a high signal-to-noise ratio. With this method, after having once acquired a transmitted signal (by manual search across the expected frequency re-

TABLE 4. SUMMARY OF NOTS I TEST RESULTS

Test Purpose	Date of Test	Missile	Observed Results	Cause of Failure
Performance of 2nd-stage motor under acceleration. Partial test of structural integrity.	4 July 1958	Live 2nd stage only, empty 1st stage, early airframe structural design	One HOTROC motor blew up at 0.7 sec, causing breakup of vehicle. Other HOTROC blew up at 1.0 sec	Failure of HOTROC motor due to crack in grain probably present prior to ignition. Other HOTROC failed due to collision with weight simulating stage 3 after breakup of vehicle
Performance of 2nd-stage motor under acceleration, structural adequacy, ballistic data.	18 July 1958	Live 2nd stage only, empty 1st stage, structurally like orbital missile.	Missile blew up on launcher at about +0 sec	Cause of premature ignition unknown but possible spurious pulse in lead lines to igniter or RF from doppler radar. One HOTROC motor blew up at ignition causing chamber damage to other motor and subsequent failure after 0.1 to 0.2 sec. Probable excessive charge in experimental igniter caused blowup
Orbital attempt No. 1	25 July 1958	Complete missile, diagnostic payload	Photo coverage very poor and from rear only. Missile performed violent spiral maneuver about 0.5 sec after ignition and probably broke up	Unknown. Frequency of spiral such that entire missile was probably not involved. Impossible to tell if both motors ignited
Orbital attempt No. 2	12 Aug 1958	Complete missile, diagnostic payload	Motor blowup at ignition causing general breakup of missile	Unknown. Possible cracked grain or undersize perforation
Performance of 1st stage motor under acceleration, structural adequacy, ballistic data	16 Aug 1958	Live 1st stage only, structurally like orbital missile	Missile operated normally for about 3.2 sec. Fins broke off one by one during one revolution, missile yawed to almost 90° and structure failed causing general breakup. HOTROC motors did not fail even after breakup	Fins failed under excessive loads due to high "q" at low altitude. Failure occurred at approx. load predicted from static load tests of fins. No damage noted to fin bases or motor chambers on recovered parts
Performance of 1st stage motor under acceleration, structural adequacy, ballistic data.	17 Aug 1958	Live 1st stage only, structurally like orbital missile	Missile operated normally for about 3.0 sec. Fins broke off one by one during single revolution, missile yawed to almost 90° and structure failed causing general breakup. HOTROC motors did not fail even after breakup	Fins failed under excessive loads due to high "q" at low altitude. Failure occurred at approx. load predicted from static load tests of fins. No damage noted to fin bases or motor chambers on recovered parts
Orbital attempt No. 3	22 Aug 1958	Complete missile, diagnostic payload	Ignition [illegible] 0.1 sec [illegible] motor. Telemetering [illegible] [illegible] Three [illegible] [illegible] were [illegible] [illegible] of data [illegible] orbital [illegible]	[illegible] observed [illegible] believed to be missile [illegible] and perhaps [illegible] missile [illegible]
Orbital attempt No. 4	[illegible] Aug 1958	Complete missile, radiation [illegible] payload	[illegible] sec of first stage burning [illegible] motor blew up and missile broke up	Possible weakness of connection between HOTROC [illegible] at nozzle end
Orbital attempt No. 5	[illegible] Aug 1958	Complete missile, radiation [illegible] payload	Missile did not ignite and [illegible]	Probable timer failure. No igniter flash observed. Since time of fall was sufficient for second stage ignition to occur [illegible] other stage igniter is suspect
Orbital attempt No. 6	[illegible] Aug 1958	Complete missile, radiation [illegible] payload	[illegible] HOTROC [illegible] ignited [illegible] [illegible] uneven thrust [illegible] stage was [illegible] [illegible] stage burning	Ignition at high altitude unreliable.

gion), a local circuit generates a good approximation of the incoming signal and the mathematics of the detection process, as indicated in Figure 39a, demonstrates that the signal-to-noise ratio is preserved. This can be contrasted to Figure 39b, where the detection process reduces the signal-to-noise ratio, especially at low signal levels.

At the completion of Operation Argus, the ground receiver stations were returned to NOTS and work has continued on increasing their portability and readiness. During one of the Atlas firings, a receiver station was put into operation within less than 4 hours after aircraft delivery of the station to the selected sites.

To support the receiver station network, NOTS used its IBM computing center to determine ephemerides for Explorer IV from the doppler data taken from the five receiving stations.

ORBITAL ATTEMPTS

Three orbital attempts employing vehicles with diagnostic payloads were made on 25 July, 12 August, and 22 August. On 25, 26, and 28 August 1958, three additional attempts were made with the scintillation counter payload aboard. All firings except the 22 August event malfunctioned during the first stage as the result of propulsion difficulties or altitude ignition problems. On the 22 August launching, crystal control of the payload transmitter frequency was lost just prior to launch. Three possible passes were recorded but a complete review of the data could not justify an orbital claim.

Table 4 summarizes the major test results in the program and recapitulates the analysis of results obtained in the six orbital attempts.

CONCLUSIONS

The difficult task of develo..g a complete aircraft-launched satellite-vehicle system and manufacturing and launching v..icles with payloads for Operation Argus was accomplished within the short span of 6 months. This included the development of three new rocket motors, high-altitude igniters, an infrared-sensing horizon trigger, and special electronic timers. The total structural weight of this vehicle was limited to 5 percent of the overall total vehicle weight.

The technique of safely launching satellite vehicles from aircraft at high altitudes in a loft maneuver was successfully demonstrated. Acceptable and reproducible initial aircraft launch conditions were obtained by the several pilots who were trained.

A world-wide network of highly successful portable microlock ground-receiver stations was built, deployed, and used to obtain valuable IGY and Explorer IV data. Some 370 telemetering records obtained by these stations while monitoring Explorer IV for a period of approximately 30 days were forwarded to the State University of Iowa. It has been reported that these data were among the most useful obtained on Explorer IV.

The NOTS-developed stations have an improved capability for rapid frequency scan and can be in operation in 3 to 4 hours from the time they are received at any given location.

An IBM program for computing satellite vehicle performance, missile tolerances, and ephemerides for satellites from doppler data has been developed and applied to the data received from Explorer IV. A six-degrees-of-freedom program study has also been completed for determination of orbital trajectories concurrently with stability studies.

It is believed that the experience gained in this program greatly enhanced the Nation's capabilities in space research and development and that many of the components developed will find a recurring application in this country's space program.

This program proves the feasibility and versatility of aircraft-launched satellite vehicles.

It is believed that with the experience gained in this program, a lightweight, inexpensive, highly reliable satellite vehicle of ordnance quality could be designed and manufactured on a short time scale.

[redacted]

DISTRIBUTION

Military Distribution Category 42

ARMY ACTIVITIES

1 Deputy Chief of Staff for Military Operations, D/A, Washington 25, D.C. ATTN: Dir. of SWSR
2 Chief of Research and Development, D/A, Washington 25, D.C. ATTN: Atomic Div.
3 Assistant Chief of Staff, Intelligence, D/A, Washington 25, D.C.
4 Chief of Engineers, D/A, Washington 25, D.C. ATTN: ENGNB
5 Chief of Engineers, D/A, Washington 25, D.C. ATTN: ENGTB
6- 7 Office, Chief of Ordnance, D/A, Washington 25, D.C. ATTN: ORDTN
8 Chief Signal Officer, D/A, Plans, Programs, and Ops. Div., Washington 25, D.C. ATTN: SIGOP-3A
9- 11 Commanding General, U.S. Continental Army Command, Ft. Monroe, Va.
12 Director of Special Weapons Development Office, Headquarters CONARC, Ft. Bliss, Tex. ATTN: Capt. Chester I. Peterson
13 President, U.S. Army Artillery Board, Ft. Sill, Okla.
14 President, U.S. Army Air Defense Board, Ft. Bliss, Tex.
15 President, U.S. Army Aviation Board, Ft. Rucker, Ala. ATTN: ATBG-DG
16 Commandant, U.S. Army Command & General Staff College, Ft. Leavenworth, Kansas. ATTN: ARCHIVES
17 Commandant, U.S. Army Air Defense School, Ft. Bliss, Tex. ATTN: Command & Staff Dept.
18 Commandant, U.S. Army Armored School, Ft. Knox, Ky.
19 Commandant, U.S. Army Artillery and Missile School, Ft. Sill, Okla. ATTN: Combat Development Department
20 Commandant, U.S. Army Aviation School, Ft. Rucker, Ala.
21 Commandant, U.S. Army Infantry School, Ft. Benning, Ga. ATTN: C.D.S.
22 Commanding General, Chemical Corps Training Comd., Ft. McClellan, Ala.
23 Commandant, USA Signal School, Ft. Monmouth, N.J.
24 Commanding Officer, Army Medical Research Lab., Ft. Knox, Ky.
25 Commanding General, U.S. Army Chemical Corps, Research and Development Comd., Washington 25, D.C.
26 Commanding Officer, Chemical Warfare Lab., Army Chemical Center, Md. ATTN: Tech. Library
27 Commanding Officer, Diamond Ord. Fuze Labs., Washington 25, D.C. ATTN: Chief, Nuclear Vulnerability Br. (230)
28 Commanding General, Aberdeen Proving Grounds, Md. ATTN: Director, Ballistics Research Laboratory
29- 30 Commanding General, U.S. Army Ord Missile Command, Redstone Arsenal, Ala.
31 Commander, Army Rocket and Guided Missile Agency, Redstone Arsenal, Ala. ATTN: Tech Library
32 Commanding General, White Sands Proving Ground, Las Cruces, N. Mex. ATTN: ORDBS-3E
33 Commander, Army Ballistic Missile Agency, Redstone Arsenal, Ala. ATTN: ORDAB-HT
34 Commanding General, Ordnance Ammunition Command, Joliet, Ill.
35 Commanding Officer, USA Signal R&D Laboratory, Ft. Monmouth, N.J.
36 Commanding General, U.S. Army Electronic Proving Ground, Ft. Huachuca, Ariz. ATTN: Tech. Library
37 Commanding General, USA Combat Surveillance Agency, 1124 N. Highland St., Arlington, Va.
38 Commanding Officer, USA, Signal R&D Laboratory, Ft. Monmouth, N.J. ATTN: Tech. Doc. Ctr., Evans Area
39 Director, Operations Research Office, Johns Hopkins University, 6935 Arlington Rd., Bethesda 14, Md.
40 Commander-in-Chief, U.S. Army Europe, APO 403, New York, N.Y. ATTN: Opot. Div., Weapons Br.

NAVY ACTIVITIES

41 Chief of Naval Operations, D/N, Washington 25, D.C. ATTN: OP-03EG
42 Chief of Naval Operations, D/N, Washington 25, D.C. ATTN: OP-75
43 Chief of Naval Operations, D/N, Washington 25, D.C. ATTN: OP-922G1
44- 45 Chief of Naval Research, D/N, Washington 25, D.C. ATTN: Code 811
46- 47 Chief, Bureau of Aeronautics, D/N, Washington 25, D.C.
48 Chief, Bureau of Ordnance, D/N, Washington 25, D.C.
49 Chief, Bureau of Ships, D/N, Washington 25, D.C. ATTN: Code 423
50 Director, U.S. Naval Research Laboratory, Washington 25, D.C. ATTN: Mrs. Katherine H. Cass
51- 52 Commander, U.S. Naval Ordnance Laboratory, White Oak, Silver Spring 19, Md.
53 Commanding Officer and Director, Navy Electronics Laboratory, San Diego 52, Calif.
54 Commanding Officer, U.S. Naval Mine Defense Lab., Panama City, Fla.
55 Commanding Officer, U.S. Naval Radiological Defense Laboratory, San Francisco, Calif. ATTN: Tech. Info. Div.
56 Commanding Officer and Director, U.S. Naval Civil Engineering Laboratory, Port Hueneme, Calif. ATTN: Code L31
57 Commanding Officer, U.S. Naval Schools Command, U.S. Naval Station, Treasure Island, San Francisco, Calif.
58 Superintendent, U.S. Naval Postgraduate School, Monterey, Calif.
59 Commanding Officer, Air Development Squadron 5, VX-5, China Lake, Calif.
60 Commandant, U.S. Marine Corps, Washington 25, D.C. ATTN: Code A03H
61 Director, Marine Corps Landing Force, Development Center, MCS, Quantico, Va.
62 Commanding Officer, U.S. Naval CIC School, U.S. Naval Air Station, Glynco, Brunswick, Ga.
63 Chief of Naval Operations, Department of the Navy, Washington 25, D.C. ATTN: OP-75
64- 70 Chief, Bureau of Naval Weapons, Navy Department, Washington 25, D.C. ATTN: RR

AIR FORCE ACTIVITIES

71 Assistant for Atomic Energy, Hq. USAF, Washington 25, D.C. ATTN: DCS/O
72 Hq. USAF, ATTN: Operations Analysis Office, Office, Vice Chief of Staff, Washington 25, D.C.
73- 74 Air Force Intelligence Center, Hq. USAF, ACS/I (AFCIN-3V1) Washington 25, D.C.
75 Director of Research and Development, DCS/D, Hq. USAF, Washington 25, D.C. ATTN: Guidance and Weapons Div.
76 Commander, Tactical Air Command, Langley AFB, Va. ATTN: Doc. Security Branch
77 Commander, Air Defense Command, Ent AFB, Colorado. ATTN: Assistant for Atomic Energy, ADLDC-A
78 Commander, Hq. Air Research and Development Command, Andrews AFB, Washington 25, D.C. ATTN: RDRWA
79 Commander, Air Force Ballistic Missile Div. Hq. ARDC, Air Force Unit Post Office, Los Angeles 45, Calif. ATTN: WDSOT
[illegible] Commander, AF Cambridge Research Center, L. G. Hanscom Field, Bedford, Mass. ATTN: CRQST-2
[illegible]- 90 Commander, Air Force Special Weapons Center, Kirtland AFB, Albuquerque, N. Mex. ATTN: Tech. Inf. & Intel. Div.
91 Commandant, School of Aviation Medicine, USAF, Randolph AFB, Tex. ATTN: Research Secretariat
92 Commander, 1009th Sp. Wpns. Squadron, Hq. USAF, Washington 25, D.C.
93- 94 Commander, Wright Air Development Center, Wright-Patterson AFB, Dayton, Ohio. ATTN: WCOSI
95- 97 Director, USAF Project RAND, VIA: USAF Liaison Office, The RAND Corp., 1700 Main St., Santa Monica, Calif.

[redacted]

58 Commander, Air Defense Systems Integration Div., L. G. Hanscom Field, Bedford, Mass. ATTN: [illegible]

59 Chief, Ballistic Missile Early Warning Project Office, 220 Church St., New York 13, N.Y. ATTN: Col. Leo V. Skinner, USAF

90 Commander, Rome Air Development Center, ARDC, Griffiss AFB, N.Y. ATTN: Documents Library, [illegible]

91 Commander, Air Technical Intelligence Center, USAF, Wright-Patterson AFB, Ohio. ATTN: AFCIN-4B1a, Library

92 Headquarters, 1st Missile Div., USAF, Vandenberg AFB, Calif. ATTN: Operations Analysis Office

OTHER DEPARTMENT OF DEFENSE ACTIVITIES

93 Director of Defense Research and Engineering, Washington 25, D.C. ATTN: Tech. Library

94 Director, Weapons Systems Evaluation Group, Room 1E880, The Pentagon, Washington 25, D.C.

95-98 Chief, Defense Atomic Support Agency, Washington 25, D.C. ATTN: Document Library

99 Commander, Field Command, DASA, Sandia Base, Albuquerque, N. Mex.

100 Commander, Field Command, DASA, Sandia Base, Albuquerque, N. Mex. ATTN: FCTG

101-105 Commander, Field Command, DASA, Sandia Base, Albuquerque, N. Mex. ATTN: FCWT

106 Commander-in-Chief, Strategic Air Command, Offutt AFB, Neb. ATTN: OAWS

107 Commander-in-Chief, EUCOM, APO 128, New York, N.Y.

ATOMIC ENERGY COMMISSION ACTIVITIES

108-110 U.S. Atomic Energy Commission, Technical Library, Washington 25, D.C. ATTN: For DMA

111-112 Los Alamos Scientific Laboratory, Report Library, P.O. Box 1663, Los Alamos, N. Mex. ATTN: Helen Redman

113-117 Sandia Corporation, Classified Document Division, Sandia Base, Albuquerque, N. Mex. ATTN: [illegible]

118-120 University of California Lawrence Radiation Laboratory, P.O. Box 808, Livermore, Calif. ATTN: Clovis G. Craig

121 Essential Operating Records, Division of Information Services for Storage at ERC-8. ATTN: John E. Dunn, Chief, Headquarters Records and Mail Service Branch, U.S. AEC, Washington 25, D.C.

122 Weapon Data Section, [illegible] Extension, Oak Ridge [illegible]

123-152 Technical Information [illegible] Oak Ridge, Tenn. (Surplus)

ADDITIONAL DISTRIBUTION

153 Commanding General, [illegible] AFB, [illegible]

154 Director, Ballistic [illegible] Proving Ground, Mary[illegible] Branch, Technical [illegible]

155 Director, Ballistic [illegible] Proving Ground, Mary[illegible] Measurements Laborat[illegible]

156 Chief of Naval Operat[illegible] ATTN: [illegible]

157 Chief of Naval Operat[illegible] ATTN: [illegible]

158 Chief of Naval Operat[illegible] ATTN: [illegible]

159 Chief, Bureau of [illegible] ATTN: [illegible]

160 Commander, U. S. Nava[illegible] [illegible], Calif [illegible]

161 Commander, U. S. [illegible] [illegible] D.C. [illegible]

162 Chief, Bureau of Ships [illegible] D.C. ATTN: [illegible]

163 Chief, Bureau of [illegible] D.C. ATTN: [illegible]

164 Office for Atomic Ener[illegible] Washington [illegible], D.C.

165 [illegible] of Communicat[illegible] [illegible], D.C.

166 Dep. Chief of Staff, [illegible] D.C., ATTN: AFCAP

167 Executive Secretary, [illegible] [illegible], Washington [illegible]

168 Executive Secretary, [illegible]

169 Director, Advanced Re[illegible] [illegible], D.C.

170 Commander, [illegible], Arl[illegible] Virginia

[redacted]